Optical Engineering

SPIEDigitalLibrary.org/oe

Tunable optical bandpass filter with multiple flat-top bands in nanostructured resonators

Jun Xie
Yuping Chen
Wenjie Lu
Xianfeng Chen

Tunable optical bandpass filter with multiple flat-top bands in nanostructured resonators

Jun Xie
Yuping Chen
Wenjie Lu
Xianfeng Chen
Shanghai Jiao Tong University
Department of Physics
The State Key Laboratory on Fiber-Optic Local Area Network
and
Advanced Optical Communication Systems
Shanghai 200240, China
E-mail: ypchen@sjtu.edu.cn

Abstract. Based on second-order nonlinearity, we present a tunable optical bandpass filter at *c*-band by introducing a back quasiphase-matching technique with a nanostructured named multiple resonator waveguide. Two injecting forward lights and one backward propagating light interact with difference frequency generation. At that juncture, the transmission of the forward signal can be modulated via changing the forward control power. As a result, a tunable optical bandpass filter with multiple flat-top transmit bands of the forward signal can be formed in the waveguide.
 [DOI: 10.1117/1.3552697]

Subject terms: optical devices; filtering; nonlinear optics; optical design.

Paper 100848R received Oct. 15, 2010; revised manuscript received Dec. 21, 2010; accepted for publication Jan. 17, 2011; published online Mar. 23, 2011.

1 Introduction

The optical bandpass filter is an important device of optical and electro-optical technology. It controls spectral energy in applications ranging from spectrometry to optical communication systems. It is widely used in wavelength-division multiplexing, infrared radiation detection, infrared hot-electron transistor, single frequency fiber laser, and multispectral imaging,[1–6] etc. While in optical communication, it is applied to the separate signal light at a specific wavelength from the other lights, or select some predicted wavelength band by absorbing, reflecting, or scattering other unneeded wavelengths. However, most bandpass filters only have a single narrow band, which limits their applications. With the development of all-optical networks, optical bandpass filters with several bandwidth windows and flat-top bands have attracted more attentions[7] in an all-optical network system.

In this paper, based on second-order nonlinearity in nanostructured resonators of optical crystal, we propose one type of optical bandpass filter using magnesium doped periodically poled lithium niobate (MgO:PPLN), which can generate three flat-top bands in the spectral profile simultaneously. It is noted that all-optical wavelength conversion is also achieved via bandpass filtering in our presented scheme, which can provide an all-optical route function and enhance multifunctional photonic integration in one optical device.

2 Basic Principle of Optical Bandpass Filter

In this paper, we focus on the idea of back-propagation frequency conversion in back quasiphase-matching (BQPM), which is utilized to study slowing down the group velocity of light beams based on second-order nonlinearity.[8] This technique can support different high transmissions of signals at different wavelength ranges simultaneously. Through modulating the transmission of multiple wavelengths by changing the power of control light, the tunable optical bandpass filter with multiple flat-top bands can be realized in the waveguide.

Figure 1 shows the schematic of the optical bandpass filter, which consists of a MgO:PPLN waveguide as the main platform. A signal light of 1550 nm is located in the *c*-band of optical communication, and the wavelength of the control light is 1600 nm,which is the key button that varies the bandwidths of filtering. In Fig. 1, the signal and control light enter into the waveguide from the left side, and the incident idler light injects from the right side. The idler is set at 730 nm, according to BQPM condition. Besides, three lights propagating in the waveguide should satisfy the quasiphase-matching (QPM) of different frequency generation (DFG), i.e., $\omega_i = \omega_s + \omega_c$, where ω_i is the frequency of idler light, ω_s is the frequency of signal light, and ω_c is the frequency of control light. Inside the two neighboring single resonator structures, light energy can be transmitted forward and reflected backward through the frequency conversion and interactional energy exchange. The large number of single resonators (SRs) make linear array to modulate propagating beams in the waveguide,[8–10] in which we call the multiple resonators (MR) waveguide, with the phase shifts between periodic positive and negative domain (see Fig. 2). In other words, the basic structure SR involves a phase shift in the sign of $\chi^{(2)}$, which microscale length is deemed as 2L.

The inset shown in Fig. 1 presents the fine structure of 3.64-cm long MR waveguide, $l = 2NL$, where l is the MR waveguide length, N is the SR population, and 2L is the unit length of SR. We consider two segments of equal length L in a SR with the reversed signs of $\chi^{(2)}$ as "phase shift" of QPM, it is equivalent to a Fabry–Perot cavity with a nonlinear mirror which introduces the phase shift of a nonlinear coefficient d_{31}. In the cavity, forward-propagating signal photons with the frequency ω_0 will be reflected as backward-propagating idler photons with the new resonant frequency $\omega_0' = \omega_0 + \omega_c$ satisfying DFG condition. These behaviors of signal light and idler light are both similar to what they propagate in the waveguide satisfying the Bragg condition. The energy flow of signal light is continuously transferred to idler light via the variation of control light power based on the phase shift structure in SR. Since the function of a large number of SRs correspond to a coupled BQPM MR, this kind of waveguide structure can engender two high reflectivity bands for the incident signal and two high transmission bands for the idler light in the spectrum, respectively.[11]

Assuming all lights to be TM polarized, a set of coupled equations for counter-propagating waves in the DFG process are derived as follows:

0091-3286/2011/$25.00 © 2011 SPIE

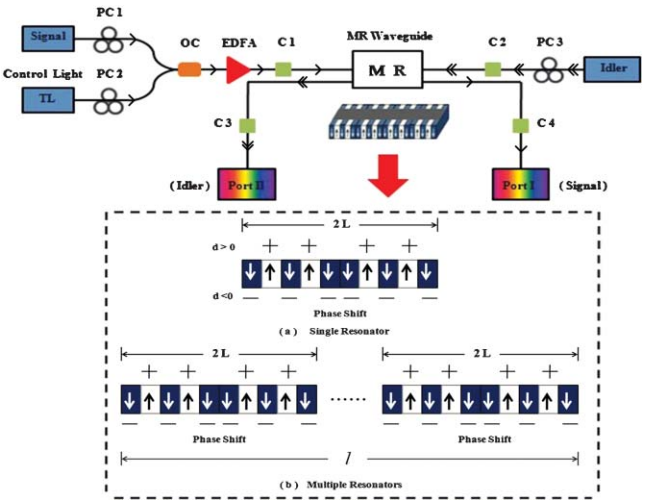

Fig. 1 Schematic diagram of tunable optical bandpass filter as MgO:PPLN MR waveguide. MR, multiple resonators, which consists of a number of single resonator (SRs); PC, polarization controller; OC, optical coupler; EDFA, erbium-doped fiber amplifier; C, collimator. The signal and idler transmit into Port I and Port II separately. Inset: the details of nanostructured resonators: (a) single resonator (SR), which is composed of a BQPM waveguide, where the sign of $\chi^{(2)}$ gets reversed periodically with one phase shift in the middle. (b) Multiple resonators (MRs), which involves a large number of SRs. In our simulation, $N = 30$, $L = 606.7\ \mu$m, and the effective transverse area of the MR waveguide: $S_w = 1\mu\text{m}^2$.

$$\frac{dA_s}{dz} = \kappa A_i e^{j2\Delta\beta z},$$
$$\frac{dA_i}{dz} = \kappa A_s e^{-j2\Delta\beta z}, \tag{1}$$

where A_s, A_i represent the electric fields of signal and idler, and the total phase mismatching is

$$\Delta\beta = \beta_s + \beta_i + \beta_c - 2\pi/\Lambda, \tag{2}$$

where β_s, β_i, β_c are the propagation constants associated with ω_s, ω_i, ω_c respectively, which are the angular frequency of signal, idler, and control lights. Λ is the poling period of BQPM.

In Eq. (1), the coupling coefficient can be expressed as

$$\kappa = \frac{4}{\pi}\frac{d_{31}}{c}\sqrt{\frac{\omega_s\omega_i}{n_s n_i n_c}\eta_0\frac{P_c}{S_w}}, \tag{3}$$

where P_c is the control power, η_0 is the vacuum impedance, S_w is the effective transverse area of waveguide, and n_s, n_i, n_c are the refractive indices of signal, idler, and control lights, respectively. In our scheme, we choose 1550 and 730 nm as the wavelength of signal light and idler light, and we understand that the grating period of 182 nm that satisfied Eq. (2), is currently too small to fabricate at our laboratory. However, precision nanoscale domain engineering of lithium niobate via UV laser induced inhibition of poling has been realized,[12] which may make the proposal of nanostructured resonators here feasible.

In order to characterize the MR waveguide structure, first, we calculated the reflection and transmission coefficients of this device as[8,13–15]

$$r = \frac{A_i(0)}{A_s(0)} = -\frac{\kappa}{s}\frac{\tanh sl}{1 + i\frac{\Delta\beta}{s}\tanh sl},$$
$$t = \frac{A_s(L)}{A_s(0)} = \frac{\cosh^{-1} sl}{1 + i\frac{\Delta\beta}{s}\tanh sl}, \tag{4}$$

where $s = \sqrt{\kappa^2 - (\Delta\beta)^2}$.

3 Multiple Flat-Top Optical Bandpass Filter

To illustrate how to realize bandpass filtering in our structure, we investigated the power of the signal, and the idler relies on the power of control light, tuning the signal from 1548 nm to 1552 nm, where the control light and idler are fixed at 1600 and 730 nm. To solve the mode matching problem in the waveguide, we can produce the idle light at 730 nm through broadband QPM second harmonic generation (SHG) by inputting 1460 nm wavelength.[16–18]

As we know, there are two types of lithium niobate (LN) waveguide in the optical communication. One is a proton-exchanged LN waveguide where Li^+ is exchanged by H^+, and the other is a titanium-diffused LN waveguide. In our scheme, we suppose that the MR waveguide of the optical filter is fabricated in 3.64-cm $LiNbO_3$ crystal by the first method-annealed proton-exchanged process. The next step is that the waveguide sample is poled by the high external electric field. Here, the PPLN waveguide sample is 3.64 cm with the effective area of waveguide as $S_w = 1\mu m^2$, and the refractive indices of the signal and idle $n_i = 2.1681$, $n_c = 2.1285$. Figure 2 shows normalized output profiles of the signal light and idler light in the MR waveguide. The cold-color region represents the low-power area, and the warm-color region means the high-power area. The power profile of the signal is divided by five areas including three red passbands and two blue forbidden bands in Fig. 2(a). In Fig. 2(b), there are three blue forbidden bands and two red passbands

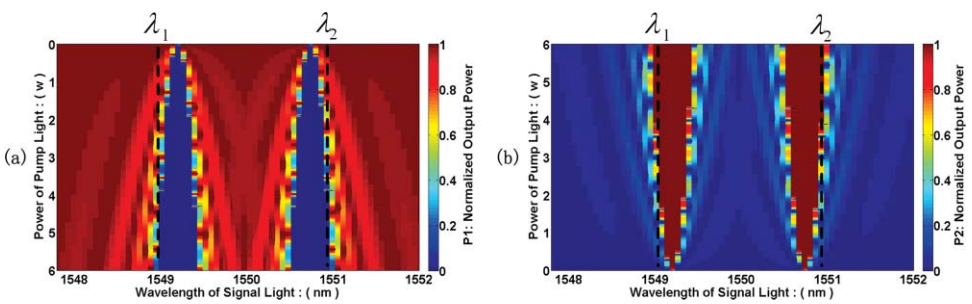

Fig. 2 Normalized output power of (a) signal light and (b) idler light with variable power of control light versus different signal wavelength, where $\lambda_1 = 1549$ nm and $\lambda_2 = 1551$ nm.

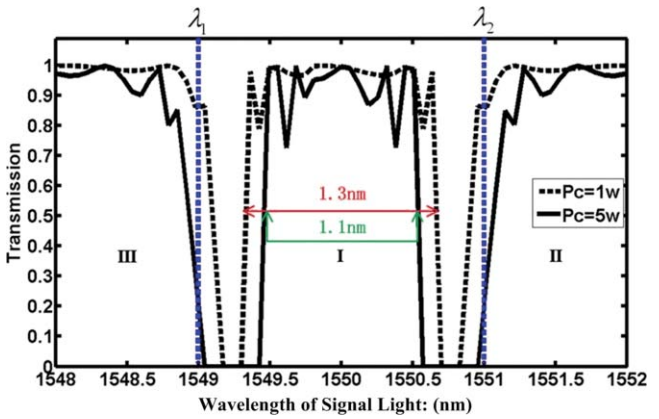

Fig. 3 Characteristic of signal light in MR waveguide at two different control powers: $P_c = 1$ W and $P_c = 5$ W.

for the idler beam according to different wavelengths of signal. With increasing the control power, the normalized output power of a signal is kept at a near zero value when the wavelength is 1550.7 or 1549.2 nm. In addition, the blue region that represents a near zero value of control power, is stretched in the signal profile. At the signals of $\lambda_1 = 1548.5$ nm and $\lambda_2 = 1551.5$ nm, their normalized output powers of signal are almost the same and equal to one [Fig. 2(a)], and the total travel range is shown respectively by the signatures of I, II, and III zones. The transition bandwidth from 1548 to 1552 nm is separated by two detect bands. Simultaneously, the normalized output power of an idler light is almost up to one at the signal of 1550.7 or 1549.2 nm [Fig. 2(b)] for the idler beam which shows the opposite behavior compared with that in Fig. 2(a). The idler is transparent at the forbidden bands of signal from 1548 to 1552 nm. It is the intrinsic principle of optical bandpass filter that the performance of signal and idler highly depends on the variation of both the wavelength of signal and the input power of the control light.

In our proposal, the power of the control light is tuned at 1 and 5 W respectively. We calculated the largest intensity of the power of control light from 1 to 5 W as 10 MW/cm^2 in MgO:PPLN waveguide. However, the light intensity without optical damage in MgO doped $LiNbO_3$ has been reported as 26 MW/cm^2 at 532 nm.[19] Thus, the power of the control light in our simulation is practicable. Figure 3 shows the transmission characteristics of signal varying the control power. Different control powers result in the variation of transmit bandwidth and forbidden bandwidth. From $P_c = 1$ W to $P_c = 5$ W, the transition and forbidden bandwidths are gradually variable within 1.3 nm $\sim$ 1.1 nm and 0.1 nm $\sim$ 0.4 nm, respectively.

Figure 4 presents the central transmission bandwidth that varies with the change of resonator nano-structures, such as the number of SR at the same waveguide length, or the length of MR waveguide at the same SR number. In Fig. 4(a), the central bandpass range is enlarged from 0.5 nm to 2.7 nm with the increase of N, the number of SR from 30 to 100 at the same MR waveguide length. Figure 4(b) shows the central transmission bandwidth decreased via increasing the MR waveguide length from $N_A = 30$ to $N_B = 50$, supposing the length of SR is fixed. The bandwidth of the central bandpass decreased from 3.5 to 0.5 nm due to the length of the MR waveguide that increased from 0.8 to 3.6 cm. The larger the length of the optical bandpass filter, the narrower the central

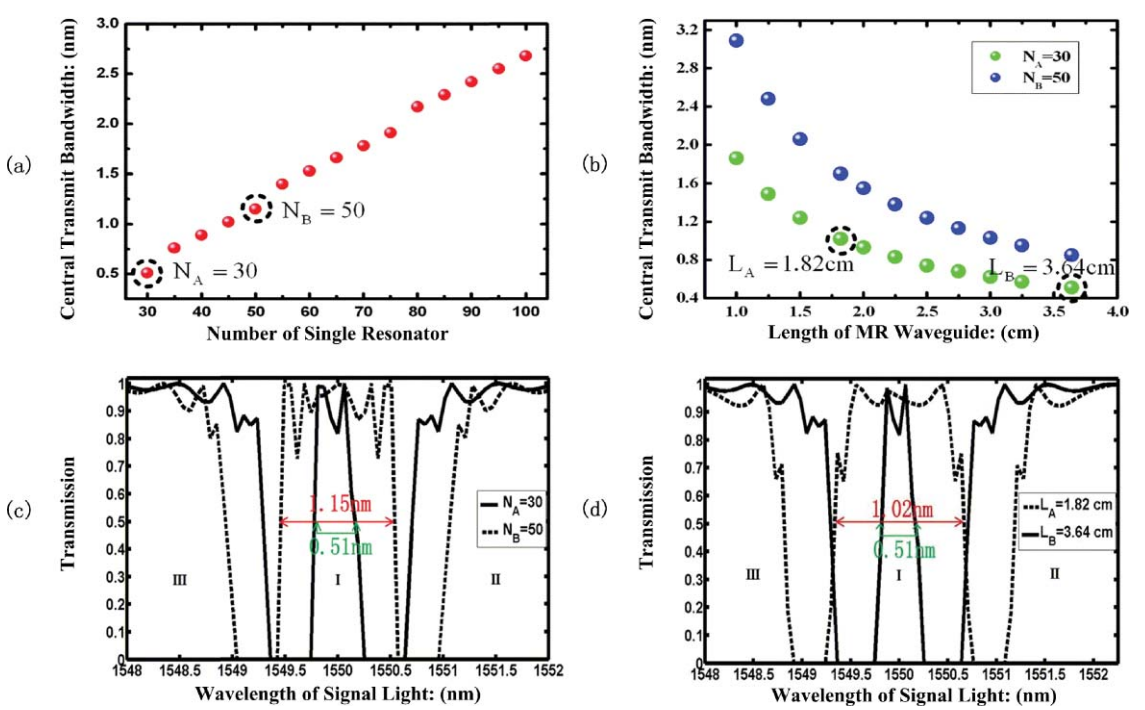

Fig. 4 (a) The central transmission bandwidth broadened with the increase of the SR number for 3.64-cm MR waveguide. (b) The central transmission bandwidth decreased via increasing MR waveguide length at different N (30 and 50). (c) At $P_c = 5$ W, simulated transmission when employing different numbers of SR: $N_A = 30$ (dotted line) and $N_B = 50$ (dashed line). (d) Simulated transmission of different lengths of MR waveguide at the same SR number N = 30: $L_A = 1.82$ cm (dotted line) and $L_B = 3.64$ cm (dashed line).

travel bandwidth we can utilize. To illustrate the function of the bandpass filter, we select specific points from Figs. 4(a) and 4(b) to calculate their transmission at different signal wavelengths in Fig. 4(c) and 4(d). In Fig. 4(c), since the central transition range is determined by the length of a single resonator,[8] we alter the numbers of SR in the same length of MR waveguide, and the transmission profiles of signal with $N_A = 30$ and $N_B = 50$ have distinct changes. In the 3.64-cm long waveguide, assuming the control power $P_c = 5\,W$, if increasing the value of N, the passbands of incident signal are filtered partially, and the forbidden bandwidths (dotted line) are broadened toward two side bands. However, the central passband range of the MR waveguide is broadened from 0.51 nm to 1.15 nm. The transmission of three flat-top passbands is entirely more than 0.8, which can make it convenient to hold the signal stable. The fabrication error of PPLN has minor effects on the results here, for the nonlinear frequency conversion efficiency of signal or idler are just proportional to the total length of the device,[18,20] which is 3.64 cm in our design. While the fabrication error is less than 1 μm, the sensitivity dependent on grating errors being 10^{-4} orders of magnitude has no influence on the filtering performance illustrated in our proposed structure.

Next, it is noted that not only one factor of the number of SRs, but also the waveguide length can impact the filtering bandwidth. Figure 4(d) shows the different central transmission bandwidth of an incident signal utilizing two different waveguide lengths $L_A = 1.82\,cm$ and $L_B = 3.64\,cm$ respectively, can be cut down from 3.44 nm (dashed line) to 0.51 nm (dotted line). The reciprocal relationship between the central bandwidth and waveguide length is revealed. Thus, the formula that indicates the central bandpass bandwidth of this filter at the same control power can be given by

$$D = \frac{C_0 \cdot N}{l}, \tag{5}$$

where D is the central bandpass bandwidth and C_0 is the material factor (here it is 6.188×10^{-13} m^2).

To improve the flexibility and tunability, we study the impact of Pockels electro-optical effect on this device further. By applying different external electric voltages on z-cut lithium niobate waveguide, the relative refractive indices between positive and negative domains can be changed according to the formula given by[21,22]

$$\begin{aligned} n_a &= n_e - \frac{1}{2}n_e^3 \cdot \gamma_{33} \cdot \frac{U}{h}, \quad \text{for positive domain,} \\ n_b &= n_e + \frac{1}{2}n_e^3 \cdot \gamma_{33} \cdot \frac{U}{h}, \quad \text{for negative domain.} \end{aligned} \tag{6}$$

These definite changes can shift the transmission band via imposing external electric voltage on the waveguide along the z-axis, which results in tunable a filtering function. Furthermore, to reduce the power needed in this scheme, one of the improved schemes is to enhance the nonlinear effect.

4 Conclusion

In this paper, we present a new scheme to achieve an optical bandpass filter with a BQPM technique in MgO:PPLN waveguide. We study the BQPM technique that can generate three flat-top bands in the signal spectrum. In this paper, the optical bandpass filter is based on nanostructured resonators designed according to second-order nonlinearity, which may constitute an all-optical communicational network as one cell device, which may constitute an all-optical communicational network as one cell device. We focus on our simulation and assume that three separated light beams go through the waveguide with different phenomena. Second-order quasiphase matching nonlinear conditions and the power of control light provide the key contribution to the whole scheme. In addition, we also illustrate the filtering process of our design. It is supposed to be the potential application in optical integrated circuits in the future.

Acknowledgments

This work was supported by the National High Technology Research and Development Program (863) of China (No. 2007AA01Z273), the National Natural Science Fund of China (10874120), and sponsored by the Scientific Research Foundation for the Returned Overseas Chinese Scholars, State Education Ministry.

References

1. T. Sano, T. Iwashima, M. Katayama, T. Kanie, M. Harumoto, M. Shigehara, H. Suganuma, and M. Nishimura, "Novel multichannel tunable chromatic dispersion compensator based on MEMS and diffraction grating," *IPTLEL* **15**, 1109–1110 (2003).
2. K. K. Choi, M. Dutta, R. P. Moerkirk, C. H. Kuan, and G. J. Iafrate, "Application of superlattice bandpass filters in 10μm infrared detection," *Appl. Phys. Lett.* **58**, 1533–1535 (1991).
3. M. Z. Tidrow, K. K. Choi, C. W. Farley, and F. Chang, "Multicolor infrared detection using a voltage tunable bandpass filter," *Appl. Phys. Lett.* **65**, 2996–2998 (1994).
4. C. Y. Lee, K. K. Choi, R. P. Leavitt, and L. F. Eastman, "Infrared hot-electron transistor with a narrow bandpass filter for high temperature operation," *Appl. Phys. Lett.* **66**, 90–92 (1995).
5. A. Gloag, N. Langford, K. McCallion, and W. Johnstone, "Tunable single frequency erbium fiber laser using an overlay bandpass filter," *Appl. Phys. Lett.* **66**, 3263–3265 (1995).
6. G. Themelis, J. S. Yoo, and V. Ntziachristos, "Multispectral imaging using multiple-bandpass filters," *Opt, Lett.* **33**, 1023–1025 (2009).
7. I. Petermann, S. Helmfrid, O. Gunnarsson, and L. Kjellberg, "Tunable and programmable optical bandpass filter," *J. Opt. A, Pure Appl. Opt.* **9**, 1057–1061 (2007).
8. J. B. Khurgin, "Slowing and stopping photons using backward frequency conversion in quasi-phase-matched waveguides," *Phys. Rev. A* **72**, 023810 (2005).
9. X. Gu, M. Makarov, and Y. J. Ding, "Backward second-harmonic and third-harmonic generation in a periodically poled potassium titanyl phosphate waveguide," *Opt. Lett.* **24**, 127–129 (1999).
10. C. Canalias, V. Pasiskevicius, M. Fokine, and F. Laurell, "Backward quasi-phase-matched second-harmonic generation in submicrometer periodically poled flux-grown KTiOPO4," *Appl. Phys. Lett.* **86**, 181105 (2005).
11. M. F. Yanik and S. Fan, "Stopping light all optically", *Phys. Rev. Lett.* **92**, 083901 (2004).
12. C. L. Sones, A. C. Muir, Y. J. Ying, S. Mailis, R. W. Eason, T. Jungk, Á. Hoffmann, and E. Soergel, "Precision nanoscale domain engineering of lithium niobate via UV laser induced inhibition of poling," *Appl. Phys. Lett.* **92**, 072905 (2008).
13. A. Yariv, *Optical Electronics in Modern Communications*, pp. 509–510, Oxford University, New York (1997).
14. J. B. Khurgin, "Optical buffers based on slow light in electromagnetically induced transparent media and coupled resonator structures: comparative analysis," *J. Opt. Soc. Am. B* **22**, 1062–1074 (2005).
15. A. Melloni, F. M. Hetti, and M. M. Nelli, "Linear and nonlinear pulse propagation in coupled resonator slow-wave optical structures" *Opt. Quantum Electron.* **35**, 365–379 (2003).
16. M. Gong, Y. Chen, Q. Sun, and X. Chen, "All optical wavelength broadcast based on simultaneous type-I QPM broadband SFG and SHG in MgO:PPLN," *Opt. Lett.* **35**, 2672–2674 (2010).
17. J. Zhang, Y. Chen, F. Lu, and X. Chen, "Flexible wavelength conversion via cascaded second order nonlinearity using broadband SHG in MgO-doped PPLN," *Opt. Express* **16**, 6957–6962 (2008).
18. Y. Chen, R. Wu, X. Zeng, Y. Xia, and X. Chen, "Type I quasi-phase-matched blue second harmonic generation with different polarization in periodically poled $LiNbO_3$," *Opt. Laser Technol.* **38**, 19–22 (2006).

19. Y. Kong, B. Li, Y. Chen, Z. Huang, S. Chen, L. Zhang, S. Liu, J. Xu, H. Liu, Y. Wang, W. Yan, X. Xie, X. Li, L. Shi, W. Zhang, and G. Zhang, "The highly optical damage resistance of lithium niobate crystals doping with Mg near its second threshold," in Photorefractive Effects, Materials, and Devices, Vol. 87 of OSA Trends in Optics and Photonics (Optical Society of America, 2003), paper 53.
20. Y. Kong, X. Chen, and Y. Xia, "Competition of frequency conversion and polarization coupling in periodically poled lithium niobate," *Appl.Phys. B* **91**, 479–482 (2008).
21. W. Lu, Y. Chen, X. Chen, and Y. Xia, "Group velocity modulation based on electro-optic photonic crystal with waveguide structure," *IEEE Photonics Technol. Lett.* **22**, 547–548 (2010).
22. J. Mørk and T. R. Nielsen, "On the use of slow light for enhancing waveguide properties," *Opt. Lett.* **35**, 2834–2836 (2010).

Jun Xie received his BS degree in applied physics from Suzhou University of Science and Technology (SUST), Suzhou, China, in 2007. He is currently working toward his MS degree at the department of physics, Shanghai Jiao Tong University (SJTU), Shanghai, China. He is currently with the State Key Laboratory of Advanced Optical Communication System and Networks, SJTU. His research interests include all-optical conversion, the design of noble optical devices, and group velocity control of light.